Hindawi
Journal of Function Spaces
Volume 2019, Article ID 8948570, 9 pages
https://doi.org/10.1155/2019/8948570

Research Article

Numerical Solution of Some Differential Equations with Henstock–Kurzweil Functions

D. A. León-Velasco,[1] **M. M. Morín-Castillo**,[2] **J. J. Oliveros-Oliveros**,[3] **T. Pérez-Becerra**,[3] **and J. A. Escamilla-Reyna**[3]

[1]*Departamento de Matemáticas Aplicadas y Sistemas, Universidad Autónoma Metropolitana Cuajimalpa, Mexico*
[2]*Facultad de Ciencias de la Electrónica, Benemérita Universidad Autónoma de Puebla, Mexico*
[3]*Facultad de Ciencias Físico Matemáticas, Benemérita Universidad Autónoma de Puebla, Mexico*

Correspondence should be addressed to D. A. León-Velasco; assaely86@gmail.com

Received 9 August 2019; Accepted 3 October 2019; Published 28 December 2019

Academic Editor: Ismat Beg

In this work, the Finite Element Method is used for finding the numerical solution of an elliptic problem with Henstock–Kurzweil integrable functions. In particular, Henstock–Kurzweil high oscillatory functions were considered. The weak formulation of the problem leads to integrals that are calculated using some special quadratures. Definitions and theorems were used to guarantee the existence of the integrals that appear in the weak formulation. This allowed us to apply the above formulation for the type of slope bounded variation functions. Numerical examples were developed to illustrate the ideas presented in this article.

1. Introduction

The main concern of this work consists of finding, using the Finite Element Method (FEM), the numerical solution of differential equations in which integrable Henstock–Kurzweil functions defined on the interval $[a, b]$ appear. We will say simply *HK* function. The space of these functions is denoted by $HK([a, b])$. In particular, we consider functions that are highly oscillatory near the singularity (no Lebesgue integrable). For that, some results that guarantee the applications of the FEM are necessary. As the first step, conditions that guarantee that the product of *HK* functions be an *HK* function. This is a consequence of the weak formulation of the differential equation. As the second step, numerical methods of integration for *HK* functions must be used, in particular, for the case of the highly oscillatory functions. The trapezoid and Simpson methods are commonly used for the numerical calculation of integrals. However, when the function is highly oscillatory with a singularity, the performance of these methods can diminish and for the case of *HK* functions, fail in the calculation. For that reason, it is necessary to use quadratures which can be capable to handle these difficulties. Different quadrature methods have been developed and improved for calculating the integral of functions that belong to different spaces. Some examples of these methods are the Gauss–Raudi [1], Gauss–Legendre and Gauss–Lobatto [2], Newton–Cotes (open and closed) and first kind of Gauss–Chebyshev quadrature rules [3]. In particular, the authors of [2] proposed a numerical improvement to the Gauss–Lobatto quadrature. The quadratures used in this work are the Lobatto quadrature [1, 2, 4] and the open quadrature defined for *HK* functions with a singularity [5]. The results obtained are compared with those given by the trapezoid quadrature. These three quadrature methods are described below.

Different authors have been studied differential equations for *HK* functions. In [6], considered the Schrödinger equation involving the Henstock–Kurzweil integral. The author proves the existence and uniqueness of the initial value problem for the Schrödinger equation when the function of the right side of the equation is *HK*. It is proved that the solution of the equation and its derivative belong to space ACG_* [7]. One example is shown to illustrate the application of these results, in which the solution of the problem presented belongs to $HK([a, b])$ and this example is not covered by any result using the Lebesgue integral. In [8], the Laplace transform for *HK* functions is considered on appropriated spaces to guarantee

its existence, continuity and differentiation but not examples of applications were presented in this work. In [9], the Henstock–Kurzweil integral is considered from a distributional analysis and two fixed-point theorems are presented.

This work is organized as follows: In Section 2, the basic elements of the FEM are given; in Section 3, the definition of the *HK* function and some basic results, which allow the application of the FEM, are given; in Section 4, some quadratures for *HK* functions are described; in Section 5, numerical examples are presented in order to validate the proposed methodology. Finally, in Section 6, the results and perspectives of the work are discussed.

2. Preliminars

The numerical solution of differential equations has great importance in mathematics and engineering since they appear in many applications. There are different methods for the numerical solution of differential equations such as finite differences, FEM, finite volume method. We are interested in the FEM due to the weak formulation of this method, that is, the method uses a variational problem associated to the differential equation. Since the modeling of many problems is made through the variational formulation, the application of the FEM is natural.

2.1. Weak Formulation. To illustrate the weak formulation of elliptic boundary problems and its resolution by the FEM, we consider the following problem:

Find $u(x) \in V$ such that

$$-\frac{d}{dx}\left(a(x)\frac{du}{dx}\right) + q(x)u = f, \quad 0 < x < L, \tag{1}$$

$$u(0) = 0, \tag{2}$$

$$\frac{du}{dx}(L) = 0, \tag{3}$$

where the set of admissible functions V is defined by

$$V = \left\{ v \in H^1(0,L) \middle| v(0) = \frac{dv}{dx}(L) = 0 \right\}. \tag{4}$$

The Equation (1) appears in some physical processes, for example, heat conduction or convection on a flat wall or on a bar, flow-through channels or pipes, axial deformation of bars, among others.

Note: In the analysis carried out in this work, generality is not lost if we consider $q(x) = 0$.

The weak formulation of the elliptic problem (1)–(3) is given by

$$\int_0^L a(x)u'(x)v'(x)dx = \int_0^L f(x)v(x)dx \quad \forall v \in V. \tag{5}$$

The variational problem (5) is also known as the weak form or Galerkin form of the differential equation. The linear space V is approximated by the discrete space V_h ($V_h \subset V$), defined by

$$V_h = gen\{\varphi_1, \varphi_2, \ldots, \varphi_N\}, \tag{6}$$

where φ_i are called base functions. For more details, see [10, 11].

2.2. Finite Element Method. The FEM provides a technique in which the domain is represented as a geometrical set of simple domains, that are called finite elements, which leads to a derivation of approximate functions on each element, usually algebraic polynomials that are chosen based on the characteristics of the problem that is being analyzed. The polynomials of degree one are commonly used because they are mathematically simple and easy to implement computationally.

Then, we can approximate the variational problem (5) for the following discrete variational problem:

Find $u_h \in V_h$ such that

$$\int_0^L a(x)u_h'(x)\varphi_i'(x)dx = \int_0^L f(x)\varphi_i(x)dx \quad i = 1, 2, \ldots, N, \tag{7}$$

with $u_h(x) = \sum_{j=1}^N u_j\varphi_j(x)$ where u_j denote $u_h(x_j)$.

Substituting u_h in (7), we get that the discrete variational problem is equivalent to calculate $u_1, u_2, \ldots u_N$ such that

$$\sum_{j=1}^N \left(\int_0^L a(x)\varphi_i'(x)\varphi_j'(x)dx \right) u_j = \int_0^L f(x)\varphi_i(x)dx, \tag{8}$$

which is reduced to solve a system of linear equations, where the matrix of the problem is symmetric and positive definite. The integrals in (8) can be calculated using the trapezoid or Simpson rule, when the diffusion parameter $a(x)$ and the source $f(x)$, are functions with finite energy (square integrable), that is, $\int_0^L [a(x)]^2 dx < \infty$ and $\int_0^L [f(x)]^2 dx < \infty$. These classical methods of integration can not be applied for functions in *HK* [5], therefore it is necessary to apply special quadratures for solving these integrals numerically and then to apply the finite element method for $a(x), f(x) \in HK$.

3. The Henstock–Kurzweil Integral

In this section we will present some of the most elementary and important properties of the Henstock–Kurzweil integral; specifically, we will mention some algebraic properties.

(i) Two compact subintervals $J, K \subset \mathbb{R}$ are called nonoverlapping if $\text{int}J \cap \text{int}K = \emptyset$. The length of an interval $I = [a, b]$, with $a \leq b$, is defined as

$$l(I) := b - a. \tag{9}$$

(ii) A subpartition of $[a, b]$ is a finite collection $\{I_i\}_{i=1}^n$ of nonoverlapping compact subintervals of $[a, b]$ with $I_i = [t_{i-1}, t_i]$. A partition of $[a, b]$ is a subpartition such that $[a, b] = I_1 \cup \ldots \cup I_n$.

(iii) A tagged partition (tagged subpartition) of $[a, b]$ is a set of ordered pairs $P := \{(I_i, \xi_i) : i = 1, \ldots, n\}$ such that the collection $\{I_i\}$ is a partition (subpartition) of $[a, b]$ and $\xi_i \in I_i$, where the point ξ_i is called tag associated to the subinterval I_i, for every $i = 1, \ldots, n$. We denoted by $\mathscr{P}$, the set of all tagged partitions of $[a, b]$.

(iv) A function $\delta : [a,b] \to \mathbb{R}$ is called a gauge on $[a,b]$ if $\delta(t) > 0$, for every $t \in [a,b]$.

(v) Given a gauge δ on $[a,b]$ and P a tagged partition (subpartition) of $[a,b]$, we say that P is δ-fine if

$$I_i \subseteq (\xi_i - \delta(\xi_i), \xi_i + \delta(\xi_i)), \tag{10}$$

for every $i = 1, \ldots, n$.

Definition 1. A function $f : [a,b] \to \mathbb{R}$ is Henstock–Kurzweil integrable on $[a,b]$ (briefly, HK integrable) and w is its integral if for every $\epsilon > 0$ there exists a gauge $\delta = \delta_\epsilon$ on $[a,b]$ such that for every δ-fine tagged partition $\{(I_i, \xi_i) : i = 1, \ldots, n\}$ of $[a,b]$ the inequality

$$\left| \sum_{i=1}^{n} f(\xi_i) l(I_i) - w \right| < \epsilon \tag{11}$$

holds.

The integral w is unique as a consequence of Cousin's Lemma. We denote the space of all Henstock–Kurzweil integrable functions by $HK([a,b])$ and to the value of the integral by $(HK)\int_a^b f$.

The HK integral is not an absolute integral in the sense that if $f : [a,b] \to \mathbb{R}$ is HK integrable on $[a,b]$, the function $|f|$ is not necessarily integrable on $[a,b]$ (see [7]). However, if $|f|$ is integrable we have the following:

Theorem 2. *If $f, |f| : [a,b] \to \mathbb{R}$ are HK integrable functions on $[a,b]$, then*

$$\left| (HK)\int_a^b f \right| \leq (HK)\int_a^b |f|. \tag{12}$$

The following result characterizes the integrability of a function when there is no particular value that can be predicted as the value of the integral, or it is unknown.

Theorem 3 (Cauchy's criterion). *A function $f : [a,b] \to \mathbb{R}$ is HK integrable on $[a,b]$ if and only if for every $\epsilon > 0$ there exists a gauge δ on $[a,b]$ such that for every δ-fine tagged partitions $\{(I_i, \xi_i) : i = 1, \ldots, n\}$ and $\{(J_j, \tau_j) : j = 1, \ldots, m\}$ of $[a,b]$ the inequality*

$$\left| \sum_{i=1}^{n} f(\xi_i) l(I_i) - \sum_{j=1}^{m} f(\tau_j) l(J_j) \right| \leq \epsilon \tag{13}$$

holds.

Given the relationship between the concept of measurability and integrability, as in the Lebesgue integral, we cannot ignore this concept of great relevance in this work, so in this section we will present some important results related to measurability.

Definition 4. A function $f : [a,b] \to \mathbb{R}$ is called simple on $[a,b]$ if there is a finite sequence $E_m \subset [a,b]$, $m = 1, \ldots, p$ of measurable sets such that $E_m \cap E_l = \emptyset$ for $m \neq l$ and $[a,b] = \bigcup_{m=1}^{p} E_m$ where $f(t) = y_m$ for $t \in E_m$, $m = 1, \ldots, p$, i.e. f is constant on the measurable set E_m.

Definition 5. A function $f : [a,b] \to \mathbb{R}$ is Lebesgue measurable on $[a,b]$ if and only if there exists a sequence of simple functions (s_n) on $[a,b]$ such that

$$f(t) = \lim_{n \to \infty} s_n(t), \text{ almost everywhere in } [a,b]. \tag{14}$$

Theorem 6. *If $f : [a,b] \to \mathbb{R}$ is HK integrable on $[a,b]$, then f is Lebesgue measurable on $[a,b]$.*

Definition 7. Let $f : [a,b] \to \mathbb{R}$ be a function. The variation of f on $[a,b]$ is

$$V_{[a,b]} f = \sup \left\{ \sum_{i=1}^{n} |f(x_i) - f(x_{i-1})| \,\middle|\, \{x_i\}_{i=0}^{n} \text{ is a partition of } [a,\ b] \right\}. \tag{15}$$

The function f is of bounded variation on $[a,b]$ if $V_{[a,b]} f < \infty$. The space of all bounded variation functions is denoted by $BV([a,b])$.

Definition 8. A function $F : [a,b] \to \mathbb{R}$ satisfies the Lipschitz condition if there exists $M > 0$ such that $|F(y) - F(x)| < M|y - x|$, $s, t \in [a,b]$, and F is of bounded slope variation (briefly, BSV) on $[a,b]$ if

$$\sum_{i=0}^{n-2} \left| \frac{F(t_{i+2}) - F(t_{i+1})}{t_{i+2} - t_{i+1}} - \frac{F(t_{i+1}) - F(t_i)}{t_{i+1} - t_i} \right|, \tag{16}$$

is bounded for all divisions $a = t_0 < t_1 < \cdots < t_n = b$.

The basic functions of the MEF belong to $BV([a,b])$. This fact, together with the following Theorem, guarantees that the product of functions that appear when applying the MEF is HK integrable, [7].

Theorem 9 (of Multiplication). *If $g \in HK([a,b])$ and $f \in BV([a,b])$, then $gf \in HK([a,b])$.*

Observe that in the variational formulation (5), we required the derivative of the solution u, the derivatives of the test functions v and the HK integrability of the product of these derivatives with the function $a(x)$. In [12] p. 11, an example that this product do not belongs to $HK([a,b])$ is presented. By to guarantee the existence of those integrals, the following Theorem will be used, [7].

Theorem 10. *A function F is the primitive of a function of bounded variation on $[a,b]$ if and only if F satisfies the Lipschitz condition and is of bounded slope variation on $[a,b]$.*

4. Numerical Integration for Some Henstock–Kurzweil Integrable Functions in One Dimension

The numerical integration arises from the difficulty and/or impossibility of solving analytically some integrals that are of interest to the sciences. These difficulties can be due to the integration domain, the complexity of the functions, or both. Thus, the integral of a function $f(x)$ is approximated as a finite sum of the area of rectangles of height $f(x)$ and width w_i,

$$\int_a^b f(x)dx \approx \sum_{i=1}^{n} w_i f(x_i), \tag{17}$$

which is similar to the definition of Riemann [1, 12]. To calculate the integral numerically, we need a partition of the interval $[a, b]$ of $n-1$ subintervals and then make the sum of the n values of the function $f_i = f(x_i)$ with a weight w_i. If the function f is integrable in some sense, it is expected that the sum of the right hand of (17) converge to the integral when $n \to \infty$. Different weights w_i and points x_i (called nodes) generate different integration methods [1]. Furthermore, when n grows, also the precision of the algorithm grows, except for rounding errors. In fact, the accuracy of the approximation depends strongly on the type of function $f(x)$ that we want to integrate, for example, if the function presents some singularity, it is necessary to remove it or split the interval into subintervals to avoid adding the singularity.

In the following, we consider three quadrature methods. The first is the trapezoid method, which is one of the Newton-Cotes rules more used in practice.

Trapezoid method. This quadrature is well-known and it is given by

$$\int_a^b f(x)dx \approx \frac{b-a}{2}\{f(a) + f(b)\}, \tag{18}$$

and the corresponding error is obtained from $e = -\left(f^2(\eta)/12\right)(b-a)^3$, where $\eta \in [a, b]$. The trapezoid method can be applied to a partition of the interval $[a, b]$.

As we have mentioned previously, classical integration methods can not be applied directly. The trapezoid method is not enough to solve the integral with *HK* functions. In what follows, we show three quadratures to calculate the numerical integrals of *HK* functions in one dimension.

Open quadrature. It is denoted by $Q_n^1(f)$, and it is defined as follows, [5],

$$Q_n^1(f) = \frac{b-a}{n(n+1)} \sum_{k=2}^{n} k[f(u_{n,k-1}) + f(u_{n,k})]. \tag{19}$$

This quadrature is used specially for *HK* functions with a singularity in $x = a$ in the interval $[a, b]$ since it avoids the singularity in that point.

Close quadrature. The approximation $Q_n^2(f)$ is computed as follows

$$Q_n^2(f) = \frac{b-a}{n(n+1)} \left\{ [f(u_{n,0}) + f(u_{n,1})] + \sum_{k=2}^{n} k[f(u_{n,k-1}) + f(u_{n,k})] \right\}, \tag{20}$$

this quadrature is used to solve the integral in $[a, b]$. Where, in (19) and (20), $u_{n,k}$ is defined by

$$u_{n,k} = a + \frac{k(k+1)}{n(n+1)}(b-a). \tag{21}$$

Table 1: Numerical results for the example 1 with different values of m.

m/Quadrature	$Er(u, u_h)$			
	Trapezoid	$Q^1_{n=100}$	$Q^2_{n=100}$	Lobatto
24	0.1160	0.0129	0.0133	0.0132
25	0.1105	0.0025	0.0025	0.0025
28	0.1366	0.0077	0.0076	0.0076
29	0.1600	0.0042	0.0043	0.0042
57	0.8629	0.0032	0.0032	0.0032
88	7.6738	0.0769	0.0741	0.0731
89	8.1056	0.0103	0.0102	0.0103
100	100.9334	0.0133	0.0135	0.0135
111	10.4801	0.0164	0.0167	0.0164
152	5.2819	0.1396	0.1541	0.1257
171	8.0889	0.0270	0.0293	0.0262
172	7.8753	0.1173	0.1205	0.1133
200	366.3114	4.4905	6.3352	3.0698
201	74.8573	0.9151	0.6741	0.6319

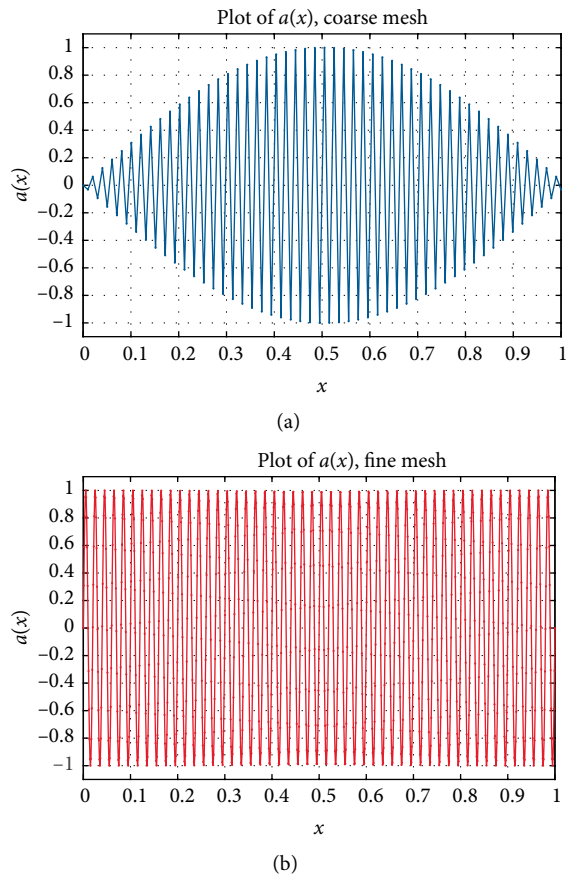

Figure 1: Diffusion parameter $a(x)$, with $m = 100$. (a) Coarse mesh ($h = 0.0101$). (b) Fine mesh ($h = 0.001001$).

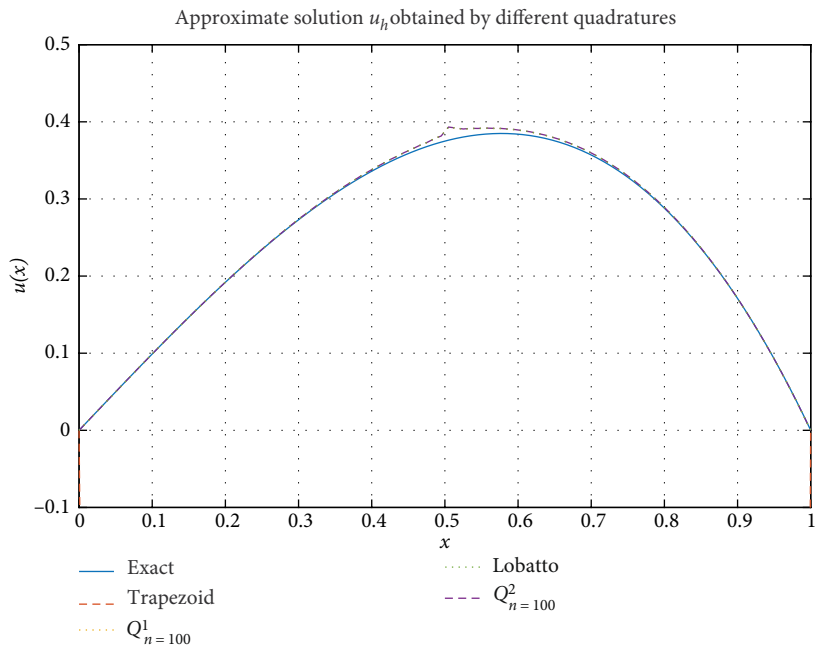

Figure 2: Exact solution $u(x)$ vs approximate solutions u_h, $m = 100$.

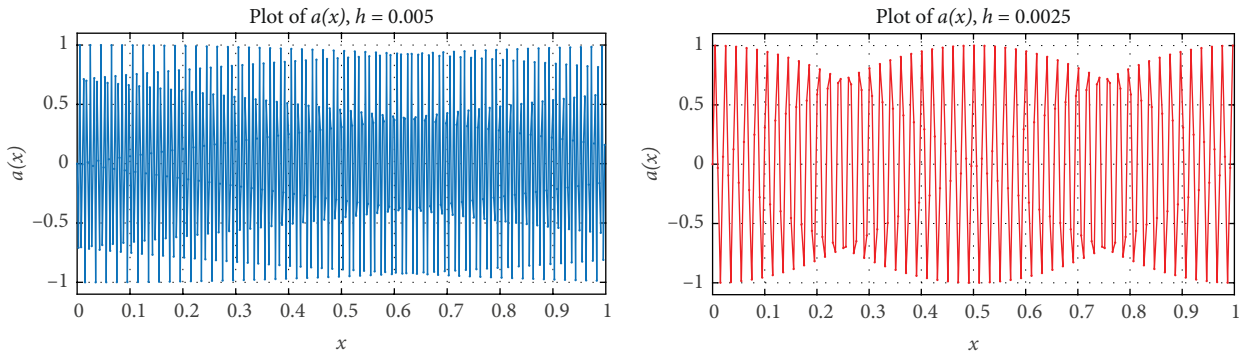

Figure 3: Diffusion parameter $a(x)$ with $m = 400$. (a) Mesh with $h = 0.00501$. (b) Mesh with $h = 0.002501$.

Table 2: Relative error for different values of m and h. Example 1.

m/Quadrature	Trapezoid	$Q^1_{n=100}$	$Q^2_{n=100}$	Lobatto
	$h = 0.00501$, 200 nodes, 199 elements			
100	0.5271	0.0403	0.0404	0.0403
200	4.9267×10^3	0.0252	0.0250	0.0251
300	5.5736	0.0695	0.0686	0.0670
400	3.6986×10^3	89.14032	43.0493	234.5809
500	6.6485	0.0307	0.0295	0.0254
1000	4.9344×10^3	0.0400	0.0235	0.0234
	$h = 0.002501$, 400 nodes, 399 elements			
100	0.0959	0.0191	0.0192	0.0191
200	0.5558	0.0157	0.0158	0.0157
300	2.3303	0.0085	0.0090	0.0087
400	2.4877×10^3	0.0119	0.0119	0.0118
500	6.4888	0.0074	0.0073	0.0076
1000	6.8514	0.0133	0.0110	0.0143

Table 3: Relative error for different meshes. Example 2.

Quadrature	$h_1 = 0.0101$	$h_2 = 0.00501$	$h_3 = 0.002501$
Trapezoid	125.2442	672.2882	0.3648
$Q^1_{n=100}$	0.2025	0.0249	0.0097
$Q^2_{n=100}$	0.0659	0.0252	0.0098
Lobatto	0.1307	0.0249	0.0097

Gauss–Lobatto. This quadrature is given by, [2],

$$\int_{-1}^{1} f(x)dx \simeq \sum_{k=1}^{n} w_i f(x_i) + pf(-1) + qf(1), \qquad (22)$$

which is exact for polynomials of degree at most $2n + 1$, nodes x_i, weights w_i and variables p and q can be determined by the undetermined coefficients method.

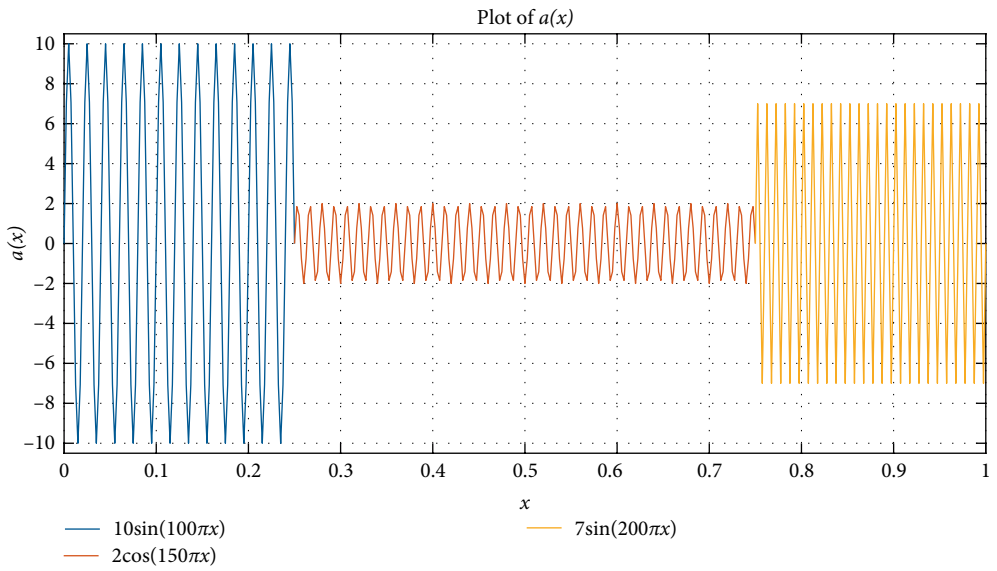

FIGURE 4: Diffusion parameter $a(x)$, with the mesh obtained by $h = 0.0025$.

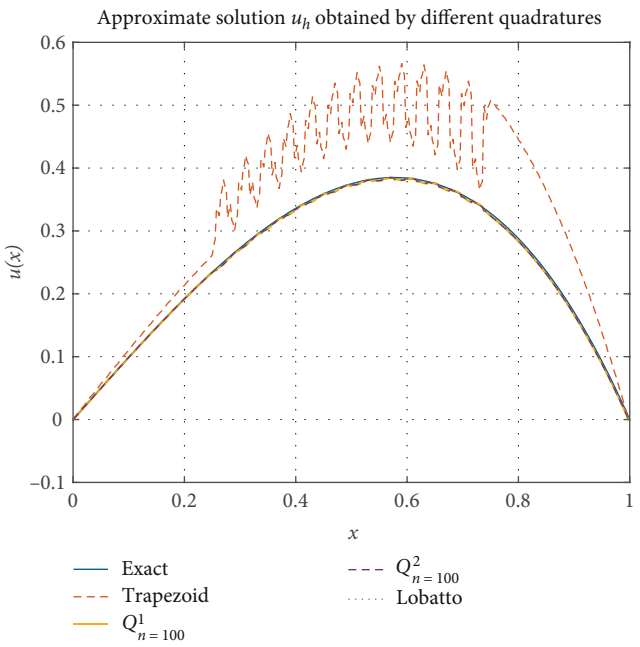

FIGURE 5: Exact solution $u(x)$ vs approximate solutions $u_h(x)$, with $h = 0.002501$.

The following result about the integration of *HK* highly oscillatory functions near of the singularity, can be found in [5].

Theorem 11. *Let* $\{x_r\} \to a^+$ *and* $A_r = lim_{n\to\infty} Q_n^1(f)$ *in* $[x_{r+1}, x_r]$, *where* $x_0 = b$. *If* $\sum_{r=0}^{\infty} A_r$ *converges, then* f *is HK integrable in* $[a, b]$ *and*

$$\int_a^b f = \sum_{r=0}^{\infty} A_r. \tag{23}$$

TABLE 4: Relative error for different meshes. Example 3.

Quadrature	$h_1 = 0.01$	$h_2 = 0.005$	$h_3 = 0.0025$	r_{h_1,h_2}	r_{h_1,h_2}
Trapezoid	—	—	—	—	—
$Q^1_{n=10}$	0.0019	2.7874×10^{-4}	1.6793×10^{-4}	2.7685	0.7316
$Q^1_{n=100}$	3.3854×10^{-4}	1.3874×10^{-4}	2.4605×10^{-5}	1.2869	2.4954
$Q^2_{n=10}$	—	—	—	—	—
$Q^2_{n=100}$	—	—	—	—	—
Lobatto	3.3807×10^{-4}	3.3075×10^{-4}	1.4451×10^{-4}	0.0316	1.1946

TABLE 5: Relative error for different meshes. Example 4, $m = 100$.

Quadrature	$h_1 = 0.0101$	$h_2 = 0.005$	$h_3 = 0.0025$
Trapezoid	1.5190	0.2337	0.0530
$Q^1_{n=100}$	0.0252	4.0611×10^{-5}	4.7206×10^{-6}
$Q^2_{n=100}$	0.0252	9.0833×10^{-5}	9.4199×10^{-5}
Lobatto	0.0255	7.5734×10^{-11}	9.6163×10^{-13}

5. Numerical Results

In this section, we present some numerical results obtained with the methodology proposed in this work. We will show how the classic methods of integration are not enough to solve elliptical differential equations with *HK*-functions. To test the convergence of the numerical results, different meshes are considered for the finite element discretization of the elliptical problems.

In order to present the numerical results, we consider the following elliptic problem:

Find $u \in V$ such that

$$-\frac{d}{dx}\left(a(x)\frac{du(x)}{dx}\right) = f, \quad 0 < x < \ell. \tag{24}$$

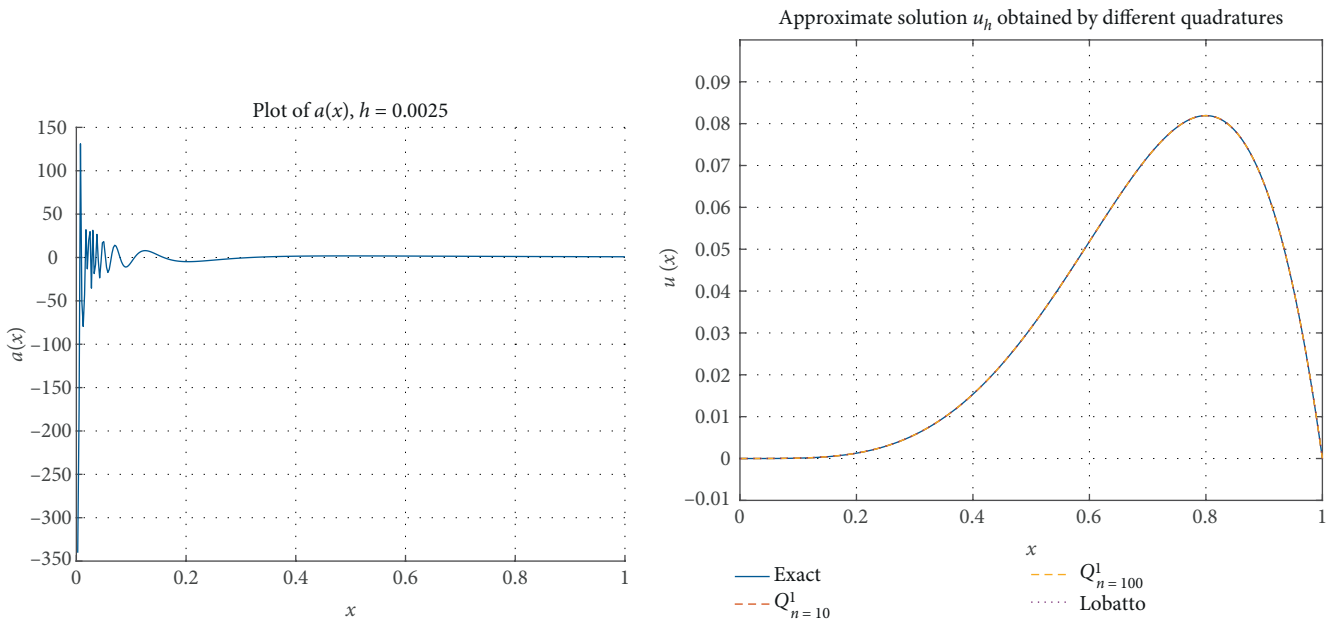

(a) (b)

FIGURE 6: (a) Diffusion parameter $a(x)$. (b) Exact solution $u(x)$ vs approximate solutions $u_h(x)$ for $h = 0.0025$.

TABLE 6: Relative error for different values of m. Example 4, $h = 0.005$.

m/Quadrature	Trapezoid	$Q^1_{n=100}$	$Q^2_{n=100}$	Lobatto
100	0.2337	4.0611×10^{-5}	9.0833×10^{-5}	7.5734×10^{-13}
150	0.6260	1.5657×10^{-4}	1.6824×10^{-4}	5.0234×10^{-11}
250	3.5168	0.0013	0.0012	1.4335×10^{-9}
300	10.1033	0.0040	0.0037	1.9332×10^{-11}
500	29.8425	0.0130	0.0123	1.5691×10^{-10}
1000	60.9681	0.0420	0.0413	0.0256

$$u(0) = 0 = u(\ell). \tag{25}$$

Also, we consider the domain $\Omega = (0, 1)$, i.e., $\ell = 1$.

Example 1. For this first example, we discretize the domain Ω with 100 nodes and 99 elements, i.e., we consider $h = 0.0101$ as the discretization parameter. We consider the diffusion parameter and the source as highly oscillating functions, given by $a(x) = \sin(m\pi x)$ and $f(x) = 6x\sin(m\pi x) - \left(1 - 3x^2\right)m\pi\cos(m\pi x)$, respectively, with $m \gg 1$ and $m \in \mathbb{N}$. The exact solution of this elliptical problem is given by $u(x) = x\left(1 - x^2\right)$.

The numerical results are summarized in Table 1, and the following relative errors are included:

$$Er(u, u_h) = \frac{\|u(x) - u_h(x)\|_{L_2(\Omega)}}{\|u(x)\|_{L_2(\Omega)}}. \tag{26}$$

These results are obtained by the FEM, where the integrals that appear in (8) are solved using the integration methods seen in the previous Section. In addition, we observe that when m increases the relative errors increase too, therefore it will be necessary to use finer meshes. We note that the trapezoid rule in not enough to obtain reasonable results, thus we have to apply special quadratures for this type of functions. Figure 1 shows the diffusion parameter in two different meshes, namely, a coarse one ($h = 0.0101$) and fine one ($h = 0.001001$), whereas Figure 2 shows the exact solution and the approximated solutions using different quadratures, with $m = 100$.

Table 2 shows the relative errors for two mesh refinement. In this Table, we observe that using special quadratures for highly oscillating functions, it is possible to obtain precision. Figure 3 shows the diffusion parameter for the two meshes, with $m = 400$.

Example 2. Now, we consider the following diffusion parameter $a(x)$, which is a continuous function defined by

$$a(x) = \begin{cases} 10\sin(100\pi x) & \text{if } 0 \le x < 0.25, \\ 2\cos(150\pi x) & \text{if } 0.25 \le x < 0.75, \\ 7\cos(200\pi x) & \text{if } 0.75 \le x < 1, \end{cases} \tag{27}$$

and the source is given by

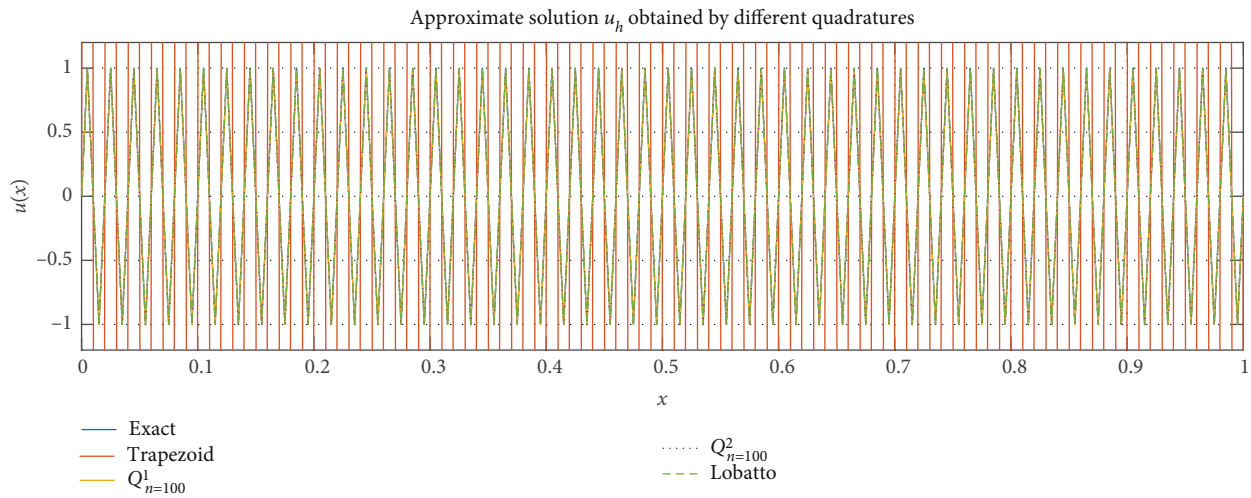

FIGURE 7: Exact solution $u(x)$ vs approximate solutions $u_h(x)$, with $m = 500$ and $h = 0.005$.

$$f(x) = \begin{cases} -1000\pi\left(1-3x^2\right)\cos(100\pi x) + 60x\sin(100\pi x) & \text{if } 0 \le x < 0.25, \\ 300\pi\left(1-3x^2\right)\sin(150\pi x) + 12x\cos(150\pi x) & \text{if } 0.25 \le x < 0.75, \\ -1400\pi\left(1-3x^2\right)\cos(200\pi x) + 42x\sin(200\pi x) & \text{if } 0.75 \le x < 1. \end{cases} \tag{28}$$

The exact solution of the differential equation (24) and (25) is $u(x) = x\left(1-x^2\right)$.

The corresponding numerical results have been summarized in Table 3, these results show convergence with the refined meshes. As in the previous example, the trapezoidal rule is not applicable for this kind of functions unless we use very refined meshes, which is very expensive computationally speaking. The diffusion parameter $a(x)$ and the approximate solutions u_h, for $h = 0.002501$, are shown in the Figures 4 and 5, respectively.

Example 3. We consider the following highly oscillatory functions with singularity in $x = 0$, $a(x) = (1/x)\sin(1/x)$ and $f(x) = x(15x-8)\sin(1/x) + (4-5x)\cos(1/x)$. The exact solution of this problem, (24) and (25), is given by $u(x) = x^4(1-x)$. To discretize Ω, we will use $h_1 = 0.01$, and two refinements, namely $h_2 = 0.005$ and $h_3 = 0.0025$.

In Table 4, the relative errors and the order of convergence obtained by three different meshes to solve the elliptic problem are shown. In this case, the trapezoid and close quadratures cannot be applicable for this kind of functions. Also, we note that the open quadrature, Q^1_n, has better convergence. In addition, for the first mesh refinement, from h_1 to h_2, we obtain convergence of second order, and convergence superlinear, for $n = 10$ and $n = 100$, respectively. Figure 6 shows the diffusion parameter $a(x)$ and the approximate solution u_h, for $h = 0.0025$.

Example 4. In this example, we use the constant diffusion parameter $a(x) = 1/10$ and the following highly oscillatory source $f(x) = 1/10(m\pi)^2\sin(m\pi x)$. The exact solution of the elliptical problem (24) and (25) is also highly oscillatory and it is given by $u(x) = \sin(m\pi x)$, with $m \gg 1$ and $m \in \mathbb{N}$. To discretize Ω we used $h_1 = 0.0101$, and two refinement of the mesh, i.e., $h_2 = 0.005$ and $h_3 = 0.0025$.

TABLE 7: Relative errors for different meshes. Example 5.

Quadrature	$h_1 = 0.01$	$h_2 = 0.005$	$h_3 = 0.0025$
Trapezoid	0.0118	0.0059	0.0029
$Q^1_{n=100}$	0.0115	0.0057	0.0029
$Q^2_{n=100}$	0.0015	0.0057	0.0029
Lobatto	0.0015	0.0057	0.0029

The relative errors for three different meshes and different quadratures, for the case $m = 100$ are summarized in Table 5. In order to apply the trapezoid method is necessary to use finer meshes, which is very expensive computationally speaking.

The numerical results reported in Table 6 have been obtained taking different values of m and $h = 0.005$. This table shows that our proposed methodology works. The exact solution and the approximate solutions, where $m = 500$ and $h = 0.005$, are shown in Figure 7. Again, we can note that the trapezoid method does not work for the highly oscillatory functions.

Example 5. For the final experiment, unlike the previous ones, let us consider homogeneous Cauchy and Neumann boundary conditions, the constant diffusion parameter $a(x) = 1$ and the source $f(x) = 1/\sqrt{x}$, that is, the only HK-function for this differential equation is $f(x)$.

$$u''(x) = \frac{1}{\sqrt{x}}, \quad 0 < x < 1, \tag{29}$$

$$u(0) = 0 = u'(1). \tag{30}$$

The exact solution of this boundary problem is given by $u(x) = (4/3)x^{3/2} - 2x$.

The results for different meshes are summarized in Table 7. In this case, the results obtained with the trapezoid

quadrature are as good as the results obtained by close, open and Lobatto quadratures.

6. Conclusions

The Finite Element Method (FEM) has been used to solve differential equations when the functions involved are continuous, or they are square-integrable. In this work, the FEM was used to solve elliptical problems where the functions involved are *HK* integrable. The numerical results, developed in the numerical examples, have shown the feasibility of FEM when special quadratures to solve these problems are used. The open quadrature and the Lobatto quadratures has shown good results. The existence and uniqueness are not studied for the problems considered in this work. These points, as well as the application to other types of *HK* functions and other types of differential equations, will be studied in future works.

Data Availability

No data were used to support this study.

Conflicts of Interest

The authors declare that they have no conflicts of interest.

Acknowledgments

The authors want to acknowledge the financial support from PRODEP through a postdoctoral scholarship for the first author. The authors acknowledge also the support from the Math Graduate program at Benemérita Universidad Autónoma de Puebla. Finally, special thanks are due to the anonymous reviewers for their valuable advice and suggestions.

References

[1] M. Masjed-Jamei, M. R. Eslahchi, and M. Dehghan, "On numerical improvement of Gauss–Radau quadrature rules," *Applied Mathematics and Computation*, vol. 168, no. 1, pp. 51–64, 2005.

[2] M. R. Eslahchi, M. Masjed-Jamei, and E. Babolian, "On numerical improvement of Gauss–Lobatto quadrature rules," *Applied Mathematics and Computation*, vol. 164, no. 3, pp. 707–717, 2005.

[3] M. Dehghan, M. Masjed-Jamei, and M. R. Eslahchi, "On numerical improvement of closed Newton–Cotes quadrature rules," *Applied Mathematics and Computation*, vol. 165, no. 2, p. 251–260, 2005.

[4] L. L. Wang and B. Y. Guo, "Interpolation approximations based on Gauss–Lobatto–Legendre–Birkhoff quadrature," *Journal of Approximation Theory*, vol. 161, no. 1, pp. 142–173, 2009.

[5] W. C. Yang, P. Y. Lee, and X. Ding, "Numerical integration on some special Henstock–Kurzweil integrals," *The Electronic Journal of Mathematics and Technology*, vol. 3, no. 3, 2009.

[6] S. Sánchez-Perales, "The initial value problem for the Schrödinger equation involving the Henstock–Kurzweil integral," *Revista de la Unión Matemática Argentina*, vol. 58, no. 2, pp. 297–306, 2017.

[7] L. P. Yee, *Lanzhou Lectures on Henstock Integration, Real Analysis*, vol. 2, World Scientific, Singapore, 1989.

[8] S. Sánchez-Perales and J. F. Tenorio, "Laplace transform using the Henstock–Kurzweil integral," *Revista de la Unión Matemática Argentina*, vol. 55, no. 1, pp. 71–81, 2014.

[9] W. Liu, G. Ye, and D. Zhao, "The distributional Henstock–Kurzweil integral and applications II," *The Journal of Nonlinear Sciences and Applications*, vol. 10, no. 1, 2017.

[10] R. Glowinski, "Finite element methods for incompressible viscous flow," in *Handbook of Numerical Analysis*, P. G. Ciarlet and J. L. Lions, Eds., vol. IX, pp. 3–1176, Amsterdam, North-Holland, 2003.

[11] S. C. Brenner and L. R. Scott, *The Mathematical Theory of Finite Element Methods*, vol. 15, Texts in Applied Mathematics, Springer, New York, 3rd edition, 2008.

[12] W. F. Pfeffer, *The Riemann Approach to Integration: Local Geometric Theory*, vol. 109, Cambridge University Press, 1993.

[13] R. Glowinski, *Variational Methods for the Numerical Solution of Nonlinear Elliptic Problems*, SIAM, Philadelphia, 2015.

[14] C. Swartz, *Measure, Integration and Function Spaces*, World Scientific, Singapore, 1994.